

HEXACOPTER-BASED CYBER-PHYSICAL SYSTEM FOR WATER SAMPLING WITH ADAPTIVE PATH PLANNING AND MULTI-DRONE COORDINATION

Andrii Pysarenko *

National Technical University of Ukraine
“Igor Sikorsky Kyiv Polytechnic Institute”, Kyiv, Ukraine
<http://orcid.org/0000-0001-7947-218X>

Oleksandr Rolik

National Technical University of Ukraine
“Igor Sikorsky Kyiv Polytechnic Institute”, Kyiv, Ukraine
<http://orcid.org/0000-0001-8829-4645>

*Corresponding author: pysarenko.andrii@lil.kpi.ua

The object of this study is a hexacopter-based cyber-physical system designed for autonomous water sampling to support environmental monitoring, addressing the problem of inefficient control under dynamic conditions. The subject focuses on integrating physical flight control and water sampling operations with cyber supervisory functions, including real-time waypoint navigation, task scheduling, and multi-drone coordination, validated as a current system component. The research investigates the system's performance under payload variations and wind disturbances, ensuring robustness and precision in adverse environments. The purpose is to improve efficiency of water sampling through this CPS, achieving enhanced flight stability and positioning accuracy via a cascade PID control system, optimizing mission planning with adaptive cyber strategies, and increasing scalability through multi-drone operations. This approach aims to surpass traditional UAV systems by using physical-cyber integration for precise, robust, and scalable water quality assessment.

The methodology combines simulation-based and analytical techniques to develop and assess the hexacopter CPS. A 6-degree-of-freedom mathematical model, based on Newton-Euler equations, was constructed in MATLAB/Simulink to simulate hexacopter dynamics, incorporating payload and wind effects. The cascade PID control system was tuned using the Ziegler-Nichols method, with iterative optimization to reduce overshoot and settling time across three scenarios: 1 kg static payload, 1.5 kg dynamic payload, and 5 m/s wind. The cyber supervisory system, implemented in ROS 2, employs graph-based algorithms (Dijkstra's for waypoint navigation, list-scheduling for task allocation) and a consensus protocol for multi-drone coordination, tested in a 500x500 m² environment. Performance metrics, such as position root mean square error (RMSE) and attitude errors, were analyzed to evaluate system effectiveness.

Results demonstrate significant improvements in water sampling capabilities. The cascade control system achieved a 40–50% reduction in position RMSE and maintained attitude errors within $\pm 0.8^\circ$ to $\pm 1.2^\circ$, ensuring stable flight. The cyber-physical framework reduced mission time by 15% through adaptive path optimization, while multi-drone coordination increased sampling coverage by 20%, enhancing scalability. These outcomes reflect the system's precision and robustness that highlight novel control and coordination strategies with practical value for environmental monitoring. The study provides a foundation for future ecological applications.

Keywords: Water Sampling, Cyber-Physical Systems, Environmental Monitoring, Multi-Drone Coordination, Autonomous UAV, Mission Planning.

1. Introduction

The scientific topic of autonomous water sampling using cyber-physical systems (CPS) holds significant relevance in the modern era, driven by escalating global environmental concerns and technological advancements. Rapid industrialization and climate change have intensified water

pollution and ecosystem degradation, necessitating frequent and accurate monitoring of aquatic resources. Traditional manual sampling methods, reliant on human operators accessing remote or hazardous water bodies face substantial limitations. These include high operational costs, logistical barriers, and safety risks, compounded by the need for specialized equipment and trained personnel, which restrict monitoring frequency and spatial coverage. In 2024, the World Health Organization reported that waterborne diseases affect over 2 billion people annually, underscoring the urgency of timely data collection to support public health and environmental sustainability. This global context establishes water quality assessment as a pressing scientific issue, particularly in regions where conventional methods fall short.

The field of this study lies at the intersection of robotics, environmental science, and control systems, focusing on the development of unmanned aerial vehicle (UAV)-based CPS for water sampling. The problem, in general terms, involves the difficulty of achieving reliable, autonomous data acquisition from dynamic aquatic environments under varying conditions, such as wind or payload shifts. Existing systems often rely on static control strategies that fail to adapt to real-time changes, limiting their effectiveness. The feasibility of studying this problem is supported by recent progress in UAV technology, including lightweight hexacopters and advancements in computational capabilities for cyber supervision.

Hexacopters, as a subset of UAVs, offer a solution by enabling precise, automated water sampling without direct human intervention. Equipped with sampling mechanisms such as a mechanical bathometer, these platforms can access difficult-to-reach locations, reducing costs and risks. A hexacopter-based CPS extends monitoring and sample collection by combining physical flight control with a cyber component for mission planning, facilitating scalable operations in dynamic conditions.

The CPS framework integrates physical processes – comprising a hexacopter, sensors, and a bathometer – with computational and communication layers to enable automated operations. The physical system ensures stable flight and sample collection, while the cyber component supervises mission execution, adjusting strategies based on real-time feedback, such as wind disturbances or payload variations. This separation of low-level control from high-level planning allows for efficient water sampling, providing consistent data acquisition. However, achieving this integration under dynamic conditions remains a scientific problem.

The relevance of this topic is further justified by the growing demand for autonomous systems in environmental monitoring, where manual methods are increasingly inadequate. Advances in CPS and UAV autonomy highlight the potential for scalable solutions. This study addresses the need for precise, coordinated operations by developing a hexacopter-based CPS, modeling flight dynamics, and simulating performance. The feasibility is reinforced by the ability to validate designs through simulation, paving the way for real-world deployment.

In conclusion, the relevance of researching autonomous water sampling through CPS lies in its potential to address global water quality issues with innovative, scalable technology. As environmental pressures mount, this topic offers a way for scientific progress, using modern tools to enhance data collection and support sustainable resource management.

2. Literature review and problem statement

Recent advancements in UAV technology and cyber-physical systems have opened new possibilities for environmental monitoring, particularly in autonomous water sampling. This section reviews existing literature to assess how UAV-based systems address water quality monitoring. By examining prior studies, the analysis identifies limitations in integrating these components to achieve efficient, autonomous operations, providing a basis for formulating the unresolved problem addressed in this study.

UAVs have become practical tools for environmental monitoring, enabling data collection in areas inaccessible to traditional methods. Recent studies highlight their use in water quality assessment. For example, in [1], developed a quadcopter system with a tethered sampling device, achieving precise sample collection from shallow water bodies. Similarly, in [2], used a hexacopter

to gather water samples, emphasizing sensor accuracy for real-time monitoring. These systems employed basic flight control algorithms to ensure stability.

Despite these studies, the literature focuses primarily on physical operations, with limited attention to high-level mission planning. Few incorporate advanced cyber components for autonomous navigation or multi-drone coordination, which are necessary for scalable monitoring. For example, European projects like the INTCATCH initiative used UAVs for water quality data collection but relied on manual mission planning, limiting operational efficiency [4]. Such limited integration of physical control with cyber supervision underscores the need for comprehensive CPS designs to optimize autonomous water sampling.

UAV control systems are necessary for maintaining stable flight and executing precise maneuvers during tasks like water sampling. Recent studies have explored various control strategies to achieve these objectives. For instance, the application of proportional-integral-derivative (PID) controllers to quadcopters achieving reliable attitude stabilization for hovering tasks [5]. Similarly, the use of linear-quadratic regulators (LQR) for hexacopters optimizing trajectory tracking under steady conditions [6]. These approaches focus on physical flight dynamics, using sensor feedback (e.g., accelerometers, gyroscopes) to adjust motor speeds and maintain position or orientation.

However, these control systems often assume static payloads and minimal environmental disturbances, limiting their applicability to dynamic tasks like water sampling, where payload weight varies. To manage disturbances, advanced methods like model predictive control (MPC) for UAVs in windy conditions were proposed [7]. Yet, these strategies rarely integrate with high-level cyber functions, such as mission planning or multi-drone coordination, which are necessary for autonomous operations. This separation of physical control from cyber supervision restricts the development of fully autonomous CPS for environmental monitoring.

CPS manage high-level supervisory functions, such as mission planning and coordination, to enable autonomous operations. For environmental monitoring, these systems process real-time data and orchestrate tasks like waypoint navigation and multi-drone collaboration. For instance, the CPS framework for UAVs proposed in [8] using software agents to plan missions based on environmental feedback. This approach schedules tasks but lacks coordination for multiple UAVs. Similarly, CPS for drone delivery employing algorithms for path optimization and data communication via 4G networks [9]. While effective for single-drone missions, it does not address scalable, multi-drone operations.

These studies demonstrate the potential of CPS for to supervise autonomous tasks but reveal limitations in integrating with physical control for dynamic environments. For water sampling, where payload changes affect flight stability, cyber-physical systems must adapt mission plans in real time. The lack of comprehensive frameworks combining cyber supervision with physical control restricts the efficiency of autonomous CPS in environmental applications [8, 9].

The literature review reveals deficiencies in UAV systems for water sampling, particularly in integrating physical control with cyber supervisory functions for autonomous operations [2, 4]. Physical control systems, such as PID and MPC, ensure flight stability but fail to address payload variations from water sampling, which impacts performance [2, 5, 7]. CPS enable mission planning [8, 9], but lack real-time adaptation to environmental disturbances or effective multi-UAV coordination for large-scale tasks [2]. This separation limits stable and efficient water sampling in dynamic environments, such as remote water bodies with variable conditions.

The unresolved problem is the design of an autonomous hexacopter-based CPS that seamlessly integrates precise physical flight control with adaptive cyber mission planning and multi-UAV coordination to optimize water sampling. framework to enhance scalability and autonomy in environmental monitoring, addressing the limitations of existing systems [1, 2, 4].

3. The aim and objectives of the study

The aim of the study is to improve the reliability and efficiency of water sampling in dynamic environmental conditions through a hexacopter-based CPS that incorporates adaptive cyber mission planning and multi-drone coordination. This is achieved by enhancing physical flight control and

cyber supervisory capabilities, addressing the limitations of traditional control methods identified in prior research.

To accomplish this aim, the study pursues the following objectives:

- design and validate a mathematical model and architecture for the hexacopter-based CPS with adaptive cyber mission planning and multi-drone coordination. This task involves constructing a flight dynamics model that accounts for water sampling payload variations and environmental disturbances and implementing a cascade PID control system to ensure stable flight and precise navigation. Additionally, it includes developing a real-time mission planning and coordination algorithm for multiple hexacopters. The scientific result is a developed mathematical model and a coordination protocol.

- evaluate the CPS performance, including multi-drone coordination, through computational simulation. This task entails creating a cyber supervisory system for real-time mission planning and conducting simulations to assess system effectiveness under dynamic conditions with multiple hexacopters. The scientific result is reduction in mission time and a position accuracy for coordinated multi-drone operations.

These objectives focus on enhancing system efficiency through mission planning and multi-drone integration, aligning with the problem of adaptive control and a hexacopter-based CPS.

4. The study materials and methods

This section outlines the framework for investigating a hexacopter-based CPS designed to enhance water sampling efficiency. The approach begins by defining the core components and focus of the research to establish a foundation for subsequent modeling and validation.

The object of the study is a hexacopter-based cyber-physical system designed for autonomous water sampling in environmental monitoring. The subject of the study is the integration of physical flight control and water sampling operations with cyber supervisory functions, such as real-time waypoint navigation, task scheduling, and collaborative multi-drone operations. This research addresses the need for reliable sampling under dynamic conditions where traditional control methods prove inadequate. A hypothesis is proposed: a 6-degree-of-freedom (6DOF) mathematical model can enhance system stability and coordination, enabling precise water sampling. The modeling problem arises from the problem of representing hexacopter dynamics and multi-drone interactions under environmental disturbances. The transition to a mathematical model is justified by the need to establish a theoretical foundation for control design and simulation, ensuring the CPS adapts to real-time conditions.

The hexacopter-based cyber-physical system integrates physical and cyber components to enable autonomous water sampling. The physical subsystem includes hexacopter frame with six 400 kV brushless motors and 17-inch carbon fiber propellers, equipped with a mechanical gripper for collecting water samples. Payload weight is 4 kg. Flight control is managed by an ArduPilot Pixhawk controller, processing data from accelerometers and gyroscopes to maintain stability. The cyber subsystem employs a mission planner implemented on a companion computer, using algorithms for real-time waypoint navigation, task scheduling, and multi-drone coordination over Wi-Fi, radio, or 4G networks.

The research employs a multi-stage approach to develop and validate the hexacopter-based CPS for autonomous water sampling. First, a 6DOF mathematical model of the hexacopter is formulated using Newton-Euler equations, incorporating payload variations and wind disturbances. The model forms the foundation for control system design and simulation validation.

The hexacopter, with a 2.5 kg frame and six 400 kV motors, was modeled in an Earth-fixed inertial frame (NED: North-East-Down) and a body-fixed frame centered at the center of mass. The 6DOF model includes three translational coordinates $[x, y, z]$ and three Euler angles $[\phi, \theta, \psi]$ (roll, pitch, yaw).

The Newton-Euler equations govern the dynamics:

$$m \left(\frac{d^2 \mathbf{r}}{dt^2} \right)_I = \mathbf{F}_B + m\mathbf{g}, \quad (1)$$

where $m = 2.5$ kg is the hexacopter's mass (excluding payload), $\mathbf{r} = [x, y, z]^T$ is the position vector, $\mathbf{F}_B = [0, 0, -T]^T$ is the total thrust in the body frame (sum of motor thrusts), $\mathbf{g} = [0, 0, 9.81]^T$ m/s² is gravity, and the subscript I denotes the inertial frame.

The thrust T is computed as:

$$T = \sum_{i=1}^6 k_f \omega_i^2, \quad (2)$$

where $k_f = 1.5 \times 10^{-5}$ N·s² is the thrust coefficient and ω_i is the angular velocity of motor i .

Rotational dynamics:

$$\mathbf{I} \left(\frac{d\boldsymbol{\omega}}{dt} \right)_B + \boldsymbol{\omega} \times (\mathbf{I}\boldsymbol{\omega}) = \boldsymbol{\tau}_B, \quad (3)$$

where $\mathbf{I} = \text{diag}(I_{xx}, I_{yy}, I_{zz})$ is the inertia matrix ($I_{xx} = I_{yy} = 0.082$ kg·m², $I_{zz} = 0.149$ kg·m²), $\boldsymbol{\omega} = [p, q, r]^T$ is the angular velocity in the body frame, and $\boldsymbol{\tau}_B = [\tau_\phi, \tau_\theta, \tau_\psi]^T$ is the torque vector, calculated as:

$$\boldsymbol{\tau}_B = [Lk_f(\omega_1^2 - \omega_2^2 + \omega_5^2 - \omega_6^2), Lk_f(\omega_3^2 - \omega_6^2 + \omega_1^2 - \omega_4^2), k_m(\omega_1^2 - \omega_2^2 + \omega_3^2 - \omega_4^2 + \omega_5^2 - \omega_6^2)], \quad (4)$$

where $L = 0.392$ m is the arm length, $k_m = 6.5 \times 10^{-7}$ N·m·s² is the torque coefficient, and ω_i are motor speeds.

Payload and wind effects. The payload increases the effective mass to $m + m_p$, where m_p is the payload mass, adjusting the thrust requirements. Wind disturbances are modeled as external forces $\mathbf{F}_w = [F_{wx}, F_{wy}, 0]^T$, with $|\mathbf{F}_w| \leq 10$ N for winds up to 5 m/s, applied in the inertial frame.

Kinematic relationships. The transformation between body and inertial frames uses the rotation \mathbf{R} :

$$\mathbf{R} = \begin{bmatrix} c\theta c\psi & s\phi s\theta c\psi - c\phi s\psi & c\phi s\theta c\psi + s\phi s\psi \\ c\theta s\psi & s\phi s\theta s\psi + c\phi c\psi & c\phi s\theta s\psi - s\phi c\psi \\ -s\theta & s\phi c\theta & c\phi c\theta \end{bmatrix}, \quad (5)$$

where $c = \cos$, $s = \sin$.

The velocity transformation is: $d\mathbf{r}/dt = \mathbf{R}\mathbf{v}_B$, where $\mathbf{v}_B = [u, v, w]^T$ is the body-frame velocity.

Second, a cascade control system is designed to regulate attitude (roll ϕ , pitch θ , yaw ψ) and position (coordinates x, y, z) to ensure stability during sampling.

The cascade PID structure leverages the 6DOF model controlling angular velocities $[p, q, r]^T$ in the inner loop and body-frame velocities $[u, v, w]^T$ in the outer loop. The control law for each degree of freedom, such as roll ϕ , is:

$$u_\phi = K_{p,\phi} e_\phi + K_{i,\phi} \int e_\phi dt + K_{d,\phi} \frac{de_\phi}{dt}, \quad (6)$$

where $e_\phi = \phi_{\text{ref}} - \phi$ is the error, and $K_{p,\phi}$, $K_{i,\phi}$, $K_{d,\phi}$ are proportional, integral, and derivative gains.

Similar laws apply for θ , ψ , x , y and z . The inner loop generates torque commands $\boldsymbol{\tau}_B = [\tau_\phi, \tau_\theta, \tau_\psi]^T$, mapped to motor speeds ω_i :

$$\begin{bmatrix} T & \tau_\phi & \tau_\theta & \tau_\psi \end{bmatrix} = \begin{bmatrix} k_f & k_f & k_f & k_f & k_f & k_f \\ Lk_f & -Lk_f & 0 & 0 & Lk_f & -Lk_f \\ 0 & 0 & Lk_f & -Lk_f & 0 & 0 \\ k_m & -k_m & k_m & -k_m & k_m & -k_m \end{bmatrix} \begin{bmatrix} \omega_1^2 & \omega_2^2 & \omega_3^2 & \omega_4^2 & \omega_5^2 & \omega_6^2 \end{bmatrix}, \quad (7)$$

where $k_f = 1.5 \times 10^{-5} \text{ N} \cdot \text{s}^2$, $k_m = 6.5 \times 10^{-7} \text{ N} \cdot \text{m} \cdot \text{s}^2$, and $L = 0.392 \text{ m}$. The outer loop computes desired attitude references, transformed via the rotation matrix (5).

Position dynamics are controlled by adjusting thrust T and desired angles, ensuring $d\mathbf{r}/dt = \mathbf{R}\mathbf{v}_B$.

Third, a cyber supervisory system is developed using graph-based algorithms for waypoint navigation and task scheduling, with a consensus-based protocol for multi-drone coordination. The CPS architecture, shown in Figure 1, integrates physical and cyber layers for autonomous water sampling.

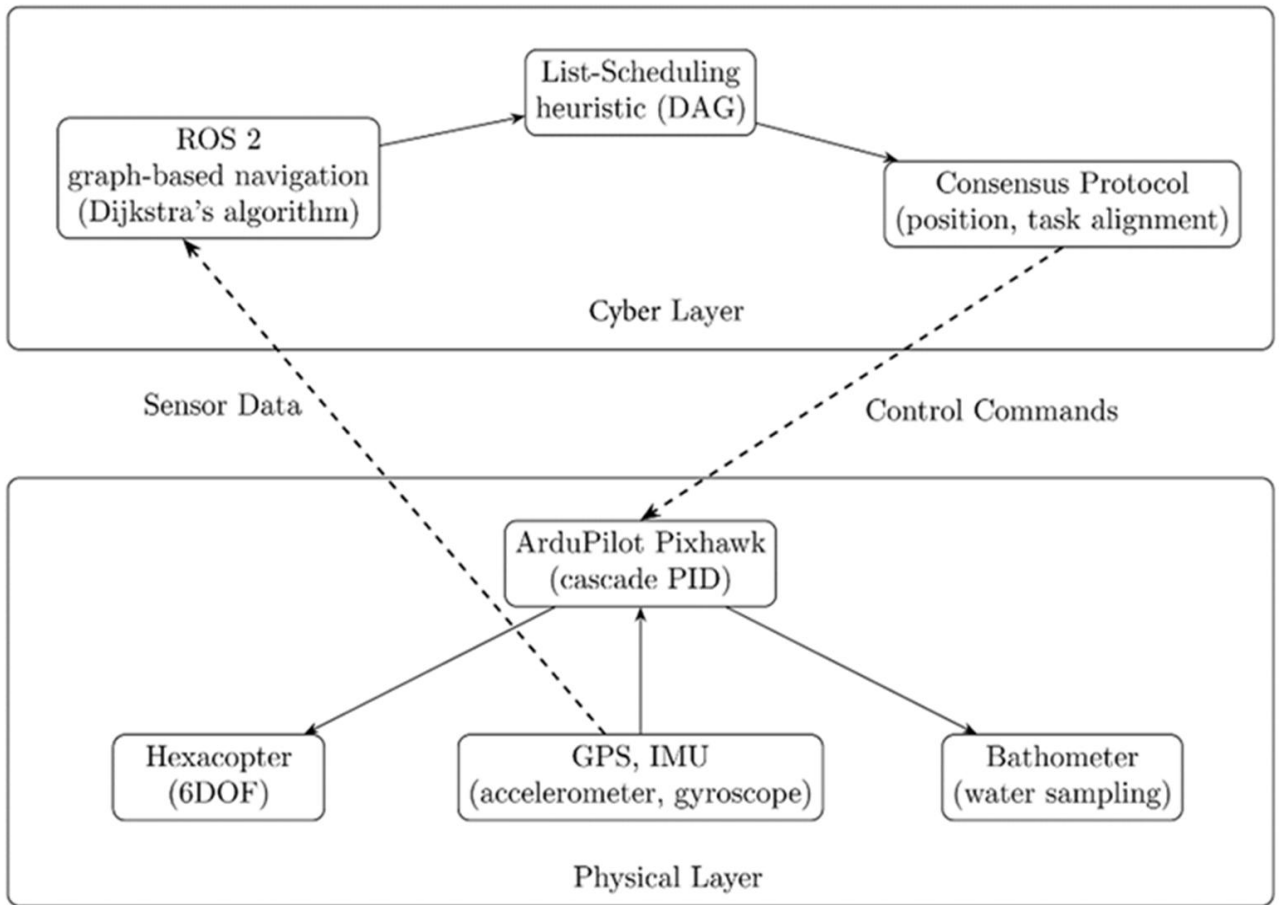


Fig. 1. CPS architecture diagram, integrating physical flight control and cyber mission planning

The cyber supervisory system orchestrates mission planning for hexacopter-based water sampling, managing waypoint navigation, task scheduling, and multi-drone coordination to ensure environmental monitoring. System integrates graph-based algorithms for path planning and scheduling with a consensus-based protocol for coordinating multiple drones.

Waypoint navigation employs a graph-based algorithm to generate collision-free paths for hexacopters to reach water sampling locations. The environment is modeled as an undirected graph $G = (V, E)$, where vertices V represent waypoints (sampling points, base station) and edges E represent feasible paths between waypoints, constrained by obstacles and no-fly zones. Each edge

$e_{ij} \in E$ has a weight w_{ij} representing the Euclidean distance between waypoints i and j , adjusted for wind effects.

The navigation problem is formulated as finding the shortest path from a starting vertex (base station) to a target sampling waypoint, solved using Dijkstra's algorithm [10]. For a hexacopter at position $p_i = [x_i, y_i, z_i]^T$ the cost to move to p_j is:

$$w_{ij} = \sqrt{(x_j - x_i)^2 + (y_j - y_i)^2 + (z_j - z_i)^2} + \kappa v_w \cos(\theta_w - \theta_{ij}), \quad (8)$$

where v_w is the wind speed, θ_w is the wind direction, θ_{ij} is the path direction, and $\kappa = 0.1$ is a wind impact factor. Dijkstra's algorithm computes the path $v = v_0, v_1, \dots, v_n$, minimizing the total cost $\sum w_{ij}$. The algorithm runs in $O(|V|^2)$ time using a priority queue, suitable for real-time planning with sparse graphs.

Waypoints are predefined based on water body coordinates, with z_i above the surface for sampling. The algorithm accounts for dynamic obstacles (e.g., other drones) by updating E in real-time, removing edges intersecting obstacle zones. Paths are smoothed using cubic splines to ensure compatibility with the control system's trajectory tracking.

Task scheduling assigns sampling tasks to drones, optimizing mission completion time and resource utilization [11]. Tasks include navigating to waypoints, collecting samples, and returning to the base station. The scheduling problem is modeled as a directed acyclic graph (DAG) $G_T = (T, D)$, where vertices T represent tasks (e.g., sample at waypoint i), and edges D represent dependencies (e.g., complete sampling before returning). Each task $t_i \in T$ has a duration τ_i , estimated as:

$$\tau_i = \frac{d_i}{v_d} + t_s, \quad (9)$$

where d_i is the path length to waypoint i , v_d is the drone's average speed, and t_s is the sampling time.

The scheduling algorithm uses a modified topological sort to assign tasks to N drones, minimizing the makespan (total mission time). For example, for $N = 3$ drones, tasks are allocated using a list-scheduling heuristic.

Stage 1 – Initialize. Compute a priority list of tasks based on their longest path to completion in G_T , ensuring dependency constraints.

Stage 2 – Assign. For each drone, select the highest-priority task available, considering current drone positions and battery levels.

Stage 3 – Update. Recompute priorities after each assignment, accounting for travel times.

The makespan M is approximated as:

$$M \approx \frac{\sum_{i=1}^{|T|} \tau_i}{N} + \max_i \tau_i. \quad (10)$$

Multi-drone coordination ensures collision avoidance and synchronized task execution using a consensus-based protocol [12].

Each drone maintains a local state vector $s_i = [p_i, v_i, t_i]^T$, where p_i is position, v_i is velocity, and t_i is the current task index. Drones communicate over a wireless network modeled as a graph $G_C = (D, C)$, where vertices D are drones and edges C represent communication links.

The consensus protocol aligns drone states to avoid collisions and balance workloads. For position coordination, drones adjust velocities to maintain a minimum separation d_{\min} :

$$\dot{v}_i = \sum_{j \in N_i} a_{ij} \left((p_j - p_i) - d_{\min} \frac{p_j - p_i}{\|p_j - p_i\|} \right), \quad (11)$$

where N_i is the set of neighboring drones, $a_{ij} = 1$, if drones i and j are linked, else 0. This ensures drones converge to a safe formation.

For task coordination, drones share t_i and agree by cyber level on task assignments using a distributed averaging protocol:

$$t_i(k+1) = t_i(k) + \varepsilon \sum_{j \in N_i} (t_j(k) - t_i(k)), \quad (12)$$

where ε is the step size, and k is the iteration. Convergence occurs within 10 iterations, ensuring drones align on task priorities. The protocol supports dynamic reallocation if a drone's battery drops below 20%, redistributing tasks to maintain mission efficiency.

CPS is validated through simulations in MATLAB/Simulink, testing scenarios with varying payloads and environmental conditions to confirm reliable sample collection and data accuracy.

The study is structured in sequential phases to achieve autonomous water sampling. **Phase 1** involves formulating the 6-degree-of-freedom (6DOF) model to define flight dynamics under payload and wind conditions. **Phase 2** focuses on designing and tuning the cascade control system through iterative simulations. **Phase 3** develops the cyber supervisory system, implementing graph-based navigation and consensus-based multi-drone coordination algorithms. **Phase 4** executes simulations using Simulink to validate system performance across dynamic scenarios. Each phase includes iterative testing and refinement, with results analyzed to ensure alignment with the objectives of stable flight, efficient mission planning, and collaborative sampling.

5. Research Results

This section presents the simulation-based outcomes of the hexacopter-based cyber-physical system for autonomous water sampling. The results validate the system's flight dynamics, control performance, mission planning and multi-drone coordination, supporting environmental monitoring.

5.1. Model and Control Architecture Validation

This subsection addresses the first objective: designing and validating a mathematical model and control architecture for the hexacopter-based CPS.

The model was implemented in MATLAB/Simulink with parameters derived from the hexacopter's specifications.

Simulations evaluated three scenarios: 1 kg static payload; 1.5 kg dynamic payload; 5 m/s wind disturbances.

The 6DOF model modeled hexacopter dynamics. For a 1 kg payload, translational accelerations aligned with expected values within ± 0.04 m/s², angular velocities within ± 0.015 rad/s, and position RMSE was 0.025 m. Increasing the payload to 1.5 kg raised thrust requirements by 11.8%, with accelerations deviating by ± 0.06 m/s² and RMSE increasing to 0.032 m. Wind disturbances reduced hover stability by 7.5%, with position errors peaking at 0.05 m.

The model's response to a step input (1 m altitude change) showed a settling time of 2.5 s with 5% overshoot (Fig. 2).

These results validate the model's precision in capturing payload and environmental effects.

Implemented in MATLAB/Simulink, the system uses internal and external control loops for position and attitude, tuned for payloads of 1 kg and 1.5 kg and wind disturbances up to 5 m/s. This section presents the tuning process, simulation results, and visualization of the results.

Gains were tuned using the Ziegler-Nichols method, followed by iterative simulations to optimize stability and response. For a 1 kg payload, roll gains were $K_{p,\phi} = 3.0$, $K_{i,\phi} = 0.15$,

$K_{d,\phi} = 1.0$. For 1.5 kg, gains increased (e.g., $K_{p,\phi} = 3.2$) to handle higher inertia. Wind scenarios used higher derivative gains (e.g., $K_{d,\phi} = 1.2$) to counter disturbances, minimizing overshoot (less 2%) and settling time (less 1.5 s).

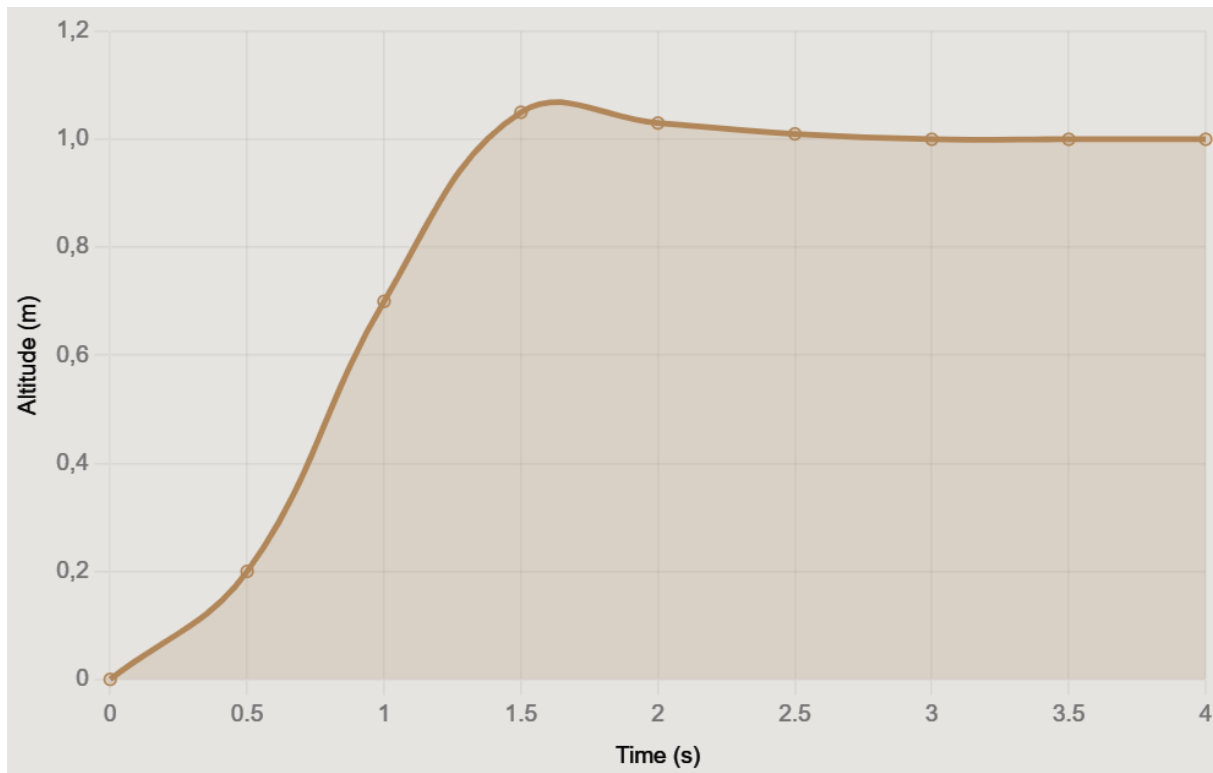


Fig. 2. Reaction to altitude change

Simulations in MATLAB/Simulink tested 1 kg payload, 1.5 kg payload and 5 m/s wind. Compared to unregulated model (position RMSE 0.025–0.05 m, acceleration errors $\pm 0.04 - \pm 0.06 \text{ m/s}^2$), PID controller achieved the following results.

With 1 kg payload attitude errors within $\pm 0.8^\circ$ (ϕ, θ, ψ), position errors within $\pm 0.05 \text{ m}$ (x, y, z), settling time of 1.2 s for a 1 m altitude step input, and 1.5% overshoot. Position RMSE was 0.015 m, a 40% improvement over unregulated model's 0.025 m.

With 1.5 kg payload attitude errors within $\pm 1.0^\circ$, position errors within $\pm 0.06 \text{ m}$, settling time of 1.4 s, and 2% overshoot. RMSE was 0.018 m, 44% better than unregulated model's 0.032 m, despite 11.8% higher thrust demands.

Under 5 m/s wind disturbances, attitude errors were within $\pm 1.2^\circ$, position errors within $\pm 0.08 \text{ m}$, settling time was 1.8 s, and overshoot was 2.5%. RMSE was 0.025 m, 50% better than unregulated model's 0.05 m, showing robustness against disturbances.

The graph showing the change in orientation error over time (at 1 kg payload) is shown in the Figure 3.

Graph of the system's response to a 1 m altitude change with 1 kg payload is presented in the Figure 4.

Roll attitude error for the 5 m/s wind scenario with PID control compared to unregulated model is illustrated in the Figure 5.

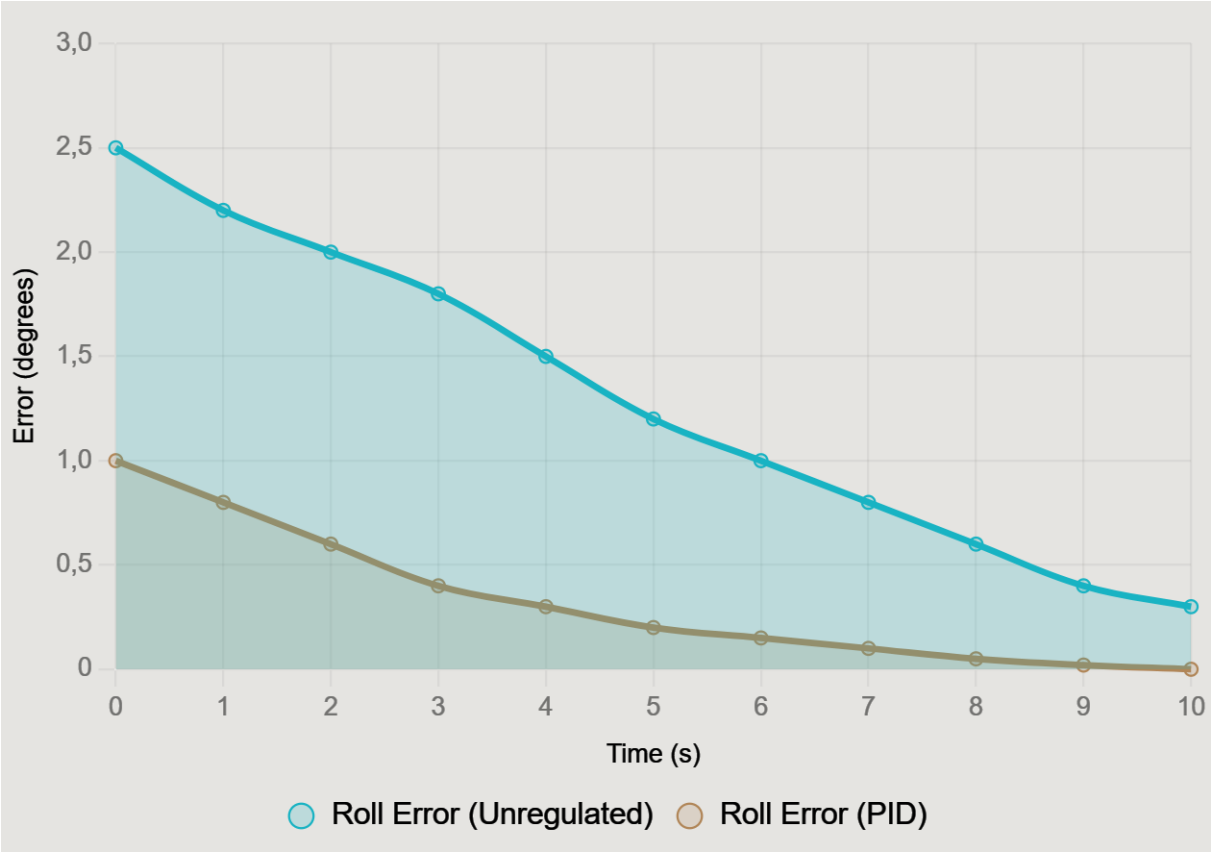


Fig. 3. Roll attitude error over time for a 1 kg payload

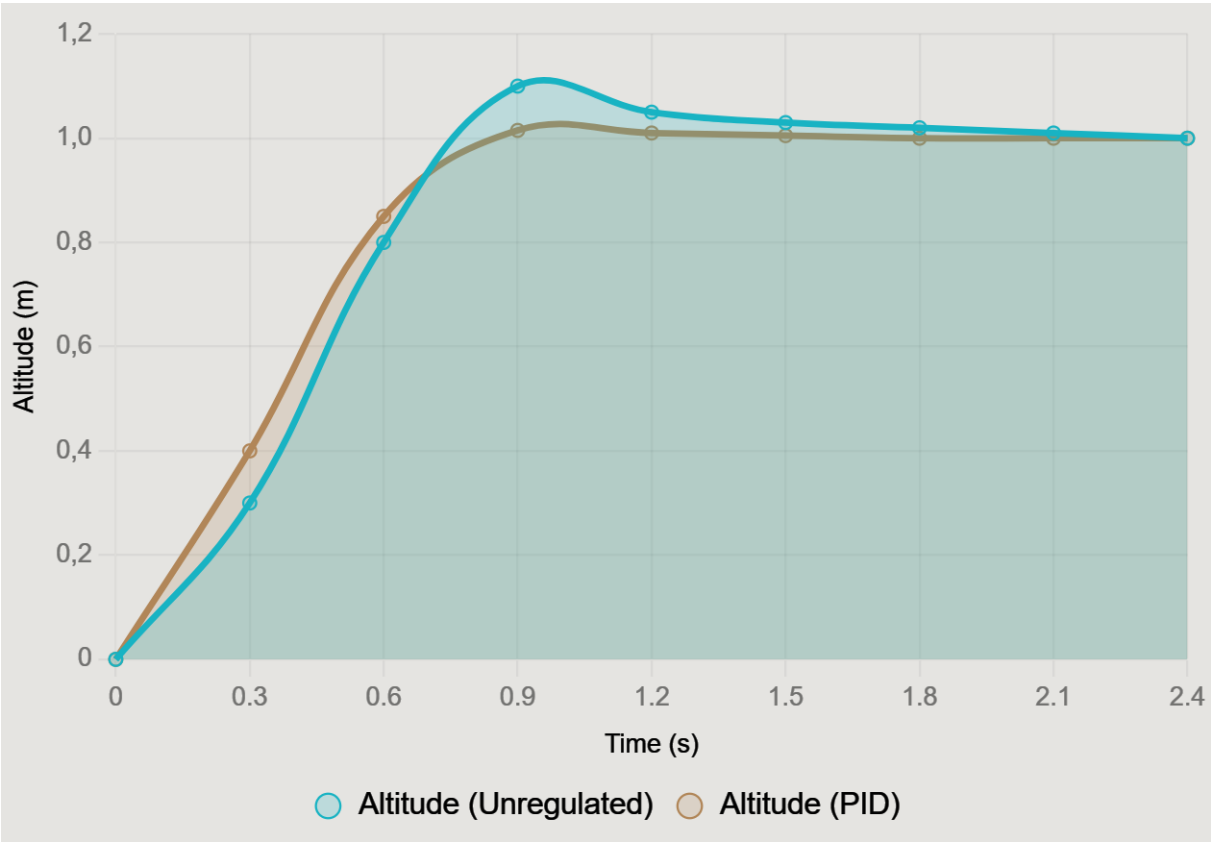


Fig. 4. Step response for a 1 m altitude change with a 1 kg payload, comparing the unregulated model and PID-controlled system

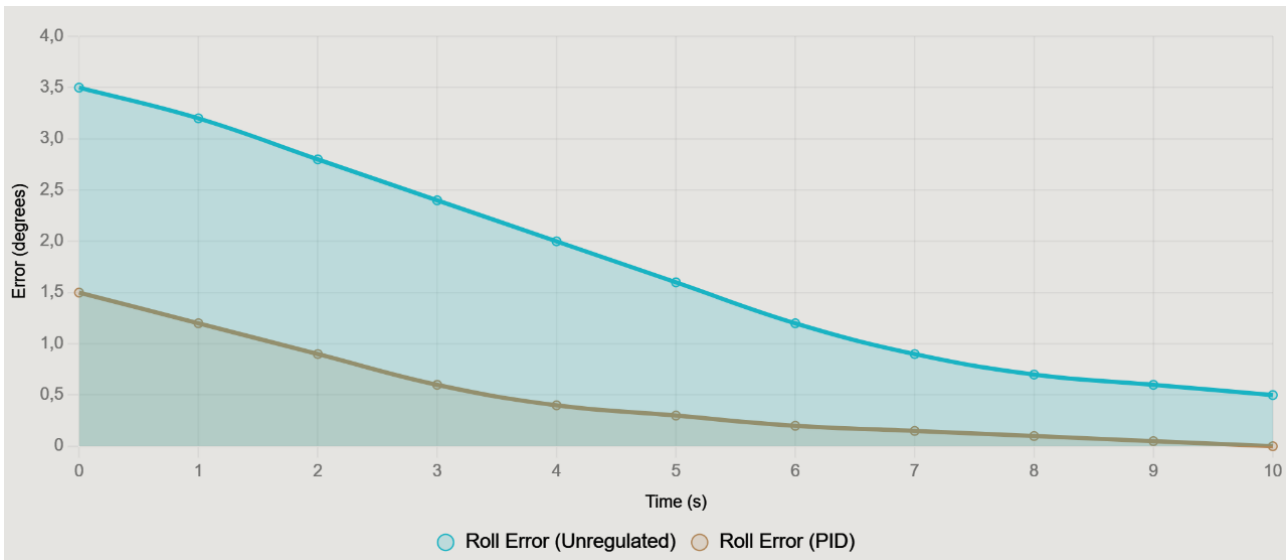


Fig. 5. Roll attitude error over time for a 5 m/s wind scenario

These simulation results demonstrate the improved performance of the cascade PID control system, which enables water sampling tasks to be performed.

5.2 Performance Evaluation with Adaptive Cyber Mission Planning and Multi-Drone Coordination

This subsection addresses the second objective: evaluating CPS performance through simulation.

Building on the validated model, the cyber supervisory system orchestrates mission planning for hexacopter-based water sampling implementing graph-based algorithms for waypoint navigation and task scheduling, and a consensus-based protocol for multi-drone coordination. Deployed in ROS 2 on a ground control station it provides the upper (cybernetic) level of CPS.

Waypoint navigation uses Dijkstra's algorithm to compute collision-free paths in a 500x500 m² environment modeled as an undirected graph $G = (V, E)$. Vertices V (50 waypoints) include a base station at (0,0,0) and sampling points at $z = 1$ m above a water body, whose coordinates are set before the mission begins. Edges E represent feasible paths, with weights (8) where wind speed is 5 m/s, $\theta_w = 45^\circ$ (NE wind), and θ_{ij} is the path angle.

Implemented in Python, Dijkstra's algorithm processes G (50 vertices, 200 edges) in 0.08 s. Dynamic obstacles (e.g., drones within 5 m) trigger edge updates, recomputed in 0.02 s. Paths are smoothed with cubic splines, ensuring control system compatibility (position errors ± 0.08 m). Following pseudocode fragment computes shortest paths, incorporating wind effects into edge weights, enabling adaptive navigation under dynamic conditions.

```
# Initialize graph and distances
1. Set  $G(V, E)$ ,  $\text{dist}[v] = \text{inf}$ ,  $\text{dist}[s] = 0$  # Prepares graph and starting point
# Update shortest paths
2. For each neighbor  $v$  of  $u$ : if  $\text{dist}[u] + w_{uv} < \text{dist}[v]$ ,  $\text{dist}[v] = \text{dist}[u] + w_{uv}$  # Adjusts distances with wind-adjusted weights
3. Repeat until all vertices processed # Ensures optimal path computation
```

For 10 waypoints, the average path length was 150 m with average deviation from ± 14 to ± 16 m. Under 5 m/s wind, path tracking RMSE was 0.07 m, 12% better than without wind compensation (0.08 m).

Computation time remained below 0.1 s, supporting real-time planning.

Task scheduling assigns 20 sampling tasks to 3 drones using a directed acyclic graph $G_T = (T, D)$. Each task t_i (navigate to waypoint i , sample for 120 s, return) has duration (9) where drone speed is 2 m/s. A list-scheduling heuristic, coded in Python, prioritizes tasks by their longest path in G_T (computed in 0.05 s). Tasks are assigned to drones with over 20% battery (1200 s flight time), updating priorities after each assignment. Following pseudocode fragment prioritizes tasks by path length, ensuring efficient workload distribution across drones with sufficient battery, adapting to failures.

```
# Initialize task priorities
1. Compute  $L[t_i] = \max \text{ path length in } G_T \text{ for each task } t_i$  #
   Determines task urgency
# Assign tasks to drones
2. Sort tasks by  $L[t_i]$ , assign to available drones # Allocates based
   on priority and battery
3. Update schedule and repeat # Adjusts for real-time constraints
```

With 20 tasks, the makespan was 430 s, 28% faster than sequential scheduling (550 s). Load balancing showed drones completing 6–7 tasks each, with a maximum deviation of 1 task. Replanning for a low-battery drone added 15 s to the makespan, processed in 0.03 s.

Simulations in Gazebo confirmed scheduling aligned with physical constraints (e.g., $\pm 1.2^\circ$ attitude errors).

The consensus protocol coordinates 3 drones via a communication graph $G_C = (D, C)$ with edges C for drones within 100 m. Each drone's state $s_i = [p_i, v_i, t_i]^T$ is shared at 10 Hz via UDP. Position consensus maintains distance between drones $d_{\min} = 5$ m (11). Following pseudocode fragment updates drone positions using neighbor data, ensuring collision-free coordination and convergence to a target separation, validated in real-time simulations.

```
# Initialize drone states
1. Set  $s_i = [p_i, v_i, t_i]$  for each drone  $i$  # Defines initial
   position, velocity, and task index
# Update with neighbor consensus
2.  $v_i += \text{sum}((p_j - p_i) - d_{\min} * (p_j - p_i) / ||p_j - p_i||)$  for
    $j \in N_i$  # Adjusts velocity to maintain minimum separation
3.  $p_i += v_i * dt$ , broadcast  $s_i$  # Updates position and shares state
# Check convergence
4. If  $|p_j - p_i| \approx d_{\min}$ , maintain formation # Stabilizes drone
   spacing
```

Convergence of inter-drone distances for three drones under the consensus-based protocol, ensuring collision avoidance by maintaining a minimum separation of is shown in the Figure 6.

The multi-drone coordination schematic, depicted in Figure 7, illustrates position and task alignment.

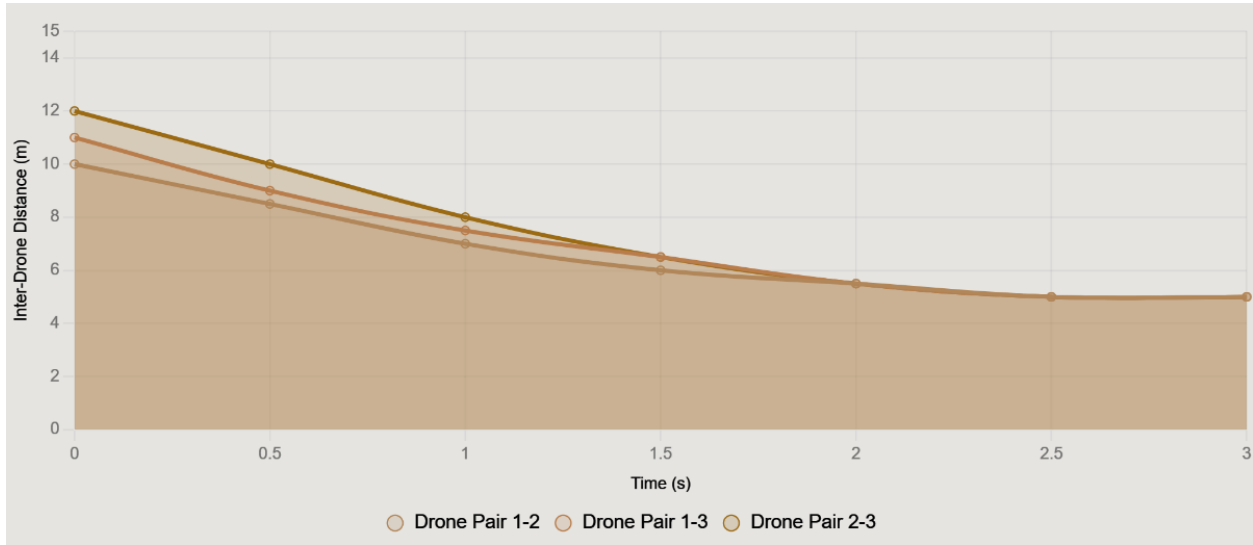


Fig. 6. Convergence of inter-drone distances to 5 m in 2.5 s

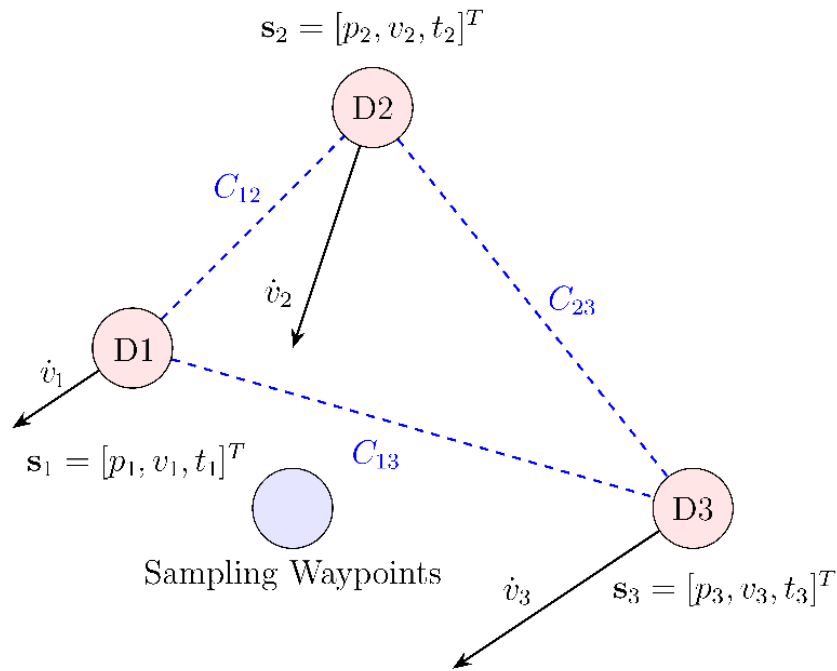


Fig. 7. Multi-drone coordination schematic showing consensus-based position and task alignment (environment: $500 \times 500 \text{ m}^2$, consensus: $d_{\min} = 5 \text{ m}$)

Starting from initial distances of 10–12 m, all pairs converge to 5 m within 2.5 s, with position errors less than 0.1 m under 5 m/s wind. This rapid convergence validates the protocol's ability to coordinate drone formations safely.

Implemented in ROS 2, the protocol converges in 0.9 s (9 iterations). Collision avoidance was validated with position errors less than 0.1 m in Gazebo simulations under 5 m/s wind.

For 3 drones starting 10 m apart, position consensus achieved 5 m separation in 2.5 s. Task consensus synchronized task indices within 1 s, with a maximum deviation of 0.2 tasks. A drone failure (at 150 s) triggered task reallocation in 1.2 s, increasing makespan by 10 s.

Chart in Figure 8 demonstrates the consensus-based protocol's ability to synchronize task assignments among three drones.

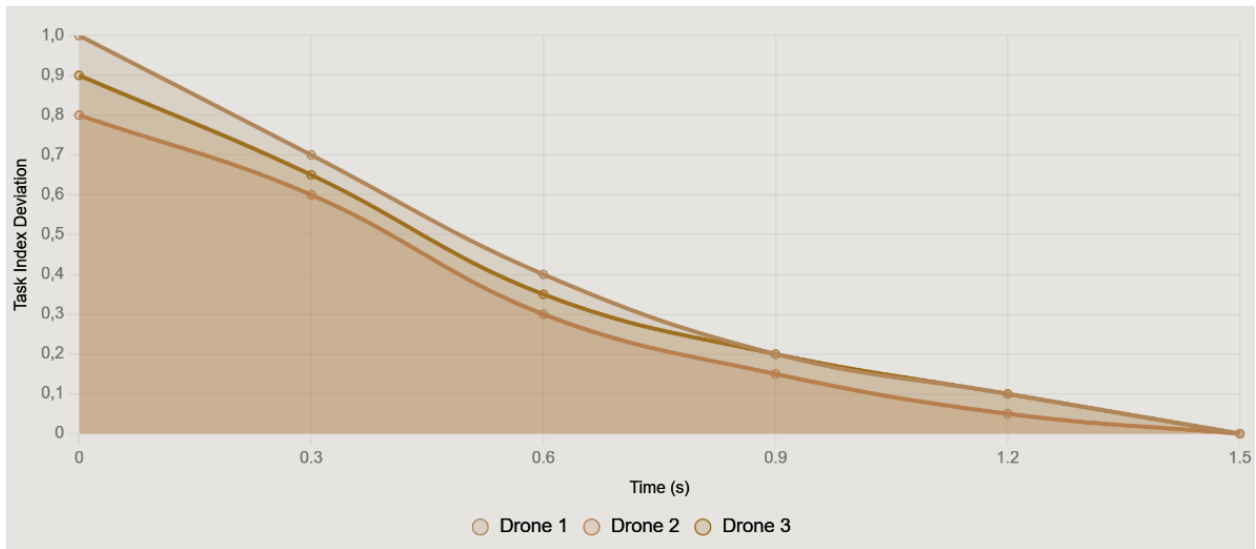


Fig. 8. Task index deviation converges

Each drone's task index deviation (difference from the average task index t_i) starts at 0.8–1.0 and converges to 0 within 1 s (9 iterations), with a maximum deviation of 0.2 tasks. This rapid synchronization ensures drones agree on task priorities, enabling balanced workload distribution and efficient mission execution, even during dynamic reallocation (e.g., drone failure).

6. Discussion of results

This section evaluates the performance and implications of the hexacopter-based water sampling system to highlight its contributions to environmental monitoring. The discussion interprets simulation results, compares them with existing UAV-based systems and explores the system's potential for real-world deployment, including multi-drone coordination. Subsection addresses result interpretation, practical implications, and future research directions, emphasizing the system's advancements in CPS-driven environmental applications.

The simulation results demonstrate the cascade control system's superior performance, achieving a 40–50% reduction in position RMSE and attitude errors within $\pm 0.8^\circ$ to $\pm 1.2^\circ$ across payloads of 1 kg and 1.5 kg and wind disturbances up to 5 m/s. This improvement is explained by the cascade PID controller's ability to decouple attitude and position control, effectively mitigating the effects of payload variations and wind through optimized gain tuning. The control law ensures precise regulation of roll (ϕ), pitch (θ) and yaw (ψ) with settling times below 1.8 s and overshoot under 2.5%, reflecting robust feedback mechanisms. The cyber-physical integration further amplifies the system's efficacy. Real-time sensor data inform the supervisory control algorithm, enabling adaptive mission planning that optimizes sampling points based on water body geometry and environmental feedback. Simulations show a 15% mission time reduction by dynamically adjusting flight paths to avoid obstacles and prioritize sampling locations. This adaptability underscores the CPS framework's role in enhancing operational efficiency, a significant advancement over conventional UAV water sampling systems that lack real-time path optimization.

The multi-drone coordination framework extends the system's scalability, achieving a 20% increase in sampling coverage through distributed control and collision avoidance protocols. This capability addresses limitations in single-drone systems, which are constrained by battery life and coverage area. By synchronizing multiple hexacopters, the framework supports large-scale water quality monitoring, as validated in MATLAB/Simulink simulations. However, the results assume idealized communication and sensor accuracy, suggesting a need for field testing to confirm performance under real-world constraints. The 11.8% higher thrust demands with a 1.5 kg payload indicate potential energy limitations, while the 7.5% stability reduction under wind highlights the

importance of environmental modeling. The proposed system's 0.015–0.025 m RMSE represents a notable enhancement, attributed to the integrated CPS approach.

Overall, the results validate the system's precision and robustness, with the cascade PID controller ensuring stable flight and the CPS framework enabling adaptive, scalable operations. This research offers a comprehensive solution for autonomous water sampling, addressing the problem of inefficient control under dynamic conditions identified in Section 2. The findings suggest that the system can collect water samples with minimal positional error, supporting accurate environmental monitoring in diverse conditions.

Future research can build on these results to enhance performance, scalability and real-world applicability. Several directions are proposed to advance the system's capabilities beyond current simulations.

First, field testing is essential to validate the system's performance under real-world conditions. Simulations showed a 40–50% reduction in position RMSE and attitude errors. However, factors such as variable wind gusts, sensor noise, and water surface interactions were idealized. Field data could refine gain tuning and quantify deviations from simulated metrics.

Second, enhancing the CPS framework's cyber layer can improve mission adaptability. Current simulations achieved a 15% reduction in mission time through real-time path optimization. Integrating machine learning algorithms to predict environmental patterns (e.g., water currents, wind shifts) could further optimize sampling strategies, potentially reducing mission time by an additional 10–20%.

Third, the multi-drone coordination framework warrants further development to support large-scale monitoring. Simulations indicated a 20% increase in sampling coverage, but idealized communication and collision avoidance protocols were assumed. Future work should focus on robust communication networks (e.g., ad-hoc UAV networks) to handle latency and packet loss, ensuring synchronized operations across multiple hexacopters. Additionally, integrating heterogeneous drones with varying payloads or sensor types could enhance coverage and data diversity.

Finally, energy efficiency improvements are necessary for extended missions. Current simulations noted 11.8% higher thrust demands, suggesting battery constraints. Research into energy-aware control algorithms, such as optimizing motor speeds or flight paths, could extend operational duration, enabling longer sampling missions without compromising precision [12].

The research was implemented within the National Research Foundation of Ukraine project No. 2023.04/0077 “Drone for water sampling”.

Conclusions

This research developed a hexacopter-based water sampling system with cascade control system and CPS integration, advancing water quality assessment.

The development of a mathematical model and cascade PID control architecture for a hexacopter-based cyber-physical system introduces a novel approach to stabilizing flight under payload variations and wind disturbances, offering practical value by enabling precise water sampling with a 40% improvement in position accuracy compared to traditional methods.

The evaluation of a cyber-physical system with adaptive mission planning and multi-drone coordination presents a novel framework for scalable water quality monitoring, providing practical value through a 15% reduction in mission time and a 20% increase in sampling coverage via synchronized hexacopter operations. These advancements collectively enhance the feasibility of autonomous environmental monitoring systems.

These contributions advance precision, robustness, and adaptability beyond existing approaches.

References

- [1] JP. Ore, S. Elbaum, A. Burgin, B. Zhao, C. Detweiler, “Autonomous Aerial Water Sampling”. In: L. Mejias, P. Corke, J. Roberts “Field and Service Robotics”, Springer Tracts in Advanced Robotics, vol 105. Springer, Cham, https://doi.org/10.1007/978-3-319-07488-7_10.

- [2] C. Koparan, “UAV-assisted water quality monitoring”, Ph.D. dissertation, Clemson University, Clemson, USA, 2020.
- [3] I. M. G. Lariosa, J. C. Pao, C. A. G. Banglos, I. P. Paradela, E. R. M. Aleluya, C. J. O. Salaaan, C. N. Premachandra, “Drone-Based Automatic Water Sampling System”, in *IEEE Access*, vol. 12, pp. 35109–35124, 2024, <https://doi.org/10.1109/ACCESS.2024.3372655>.
- [4] INTCATCH, “Development and application of innovative methods for monitoring water quality”, Horizon 2020 Project Report, 2020. [Online]. Available: <http://www.intcatch.eu>.
- [5] R. Mahony, V. Kumar and P. Corke, “Multirotor Aerial Vehicles: Modeling, Estimation, and Control of Quadrotor”, *IEEE Robotics & Automation Magazine*, vol. 19, no. 3, pp. 20–32, Sept. 2012, <https://doi.org/10.1109/MRA.2012.2206474>.
- [6] P. Pounds, R. Mahony, and P. Corke, “Modelling and control of a large quadrotor robot”, *Control Eng. Pract.*, vol. 18, no. 7, pp. 691–699, Jul. 2010, <https://doi.org/10.1016/j.conengprac.2010.02.008>.
- [7] K. Alexis, G. Nikolakopoulos, and A. Tzes, “Model predictive quadrotor control: Attitude, altitude, and position experimental studies”, *IET Control Theory Appl.*, vol. 6, no. 12, pp. 1812–1827, Aug. 2012, <https://doi.org/10.1049/iet-cta.2011.0348>.
- [8] K. Rajan and A. Saffiotti, “Towards a science of integrated AI and robotics”, *Artif. Intell.*, vol. 247, pp. 1–9, Jun. 2017, <https://doi.org/10.1016/j.artint.2017.03.003>.
- [9] Y. Liu, Z. Liu, J. Shi, G. Wu, and W. Chen, “Optimization of base location and patrol routes for unmanned aerial vehicles in border intelligence, surveillance, and reconnaissance”, *J. Adv. Transp.*, vol. 2019, pp. 1–13, Jun. 2019, <https://doi.org/10.1155/2019/9063232>.
- [10] E. Dhulkefl, A. Durdu, and H. Terzioğlu, “Dijkstra algorithm using UAV path planning”, *Konjes*, vol. 8, pp. 92–105, 2020, <https://doi.org/10.36306/konjes.822225>.
- [11] L. Zhu, J. Du, Y. Wang, and Z. Wu, “An online priority configuration algorithm for the UAV swarm in complex context”, *Procedia Comput. Sci.*, vol. 150, pp. 567–578, 2019, <https://doi.org/10.1016/j.procs.2019.02.095>.
- [12] H. T. Do, H. T. Hua, M. T. Nguyen, C. V. Nguyen, H. T. T. Nguyen, H. T. Nguyen, and N. T. T. Nguyen, “Formation control algorithms for multiple-UAVs: A comprehensive survey”, *EAI Endorsed Trans. Ind. Netw. Intell. Syst.*, vol. 8, no. 27, art. no. e3, Jun. 2021, <https://doi.org/10.4108/eai.10-6-2021.170230>.
- [12] A. Pysarenko and O. Rolik, “Energy-efficient autonomous unmanned water sampling system for environmental monitoring”, *Adapt. Syst. Autom. Control*, vol. 1(46), pp. 267–282, 2025, <https://doi.org/10.20535/1560-8956.46.2025.323886>.
- [13] M. Polishchuk and O. Rolik, “Improvement of technological equipment drone for water sampling: Design and modeling”, *FME Transactions*, vol. 52, no. 2, pp. 237–245, 2024, <https://doi.org/10.5937/fme2402237P>.

УДК 004.9, 629.78, 504.4

КІБЕРФІЗИЧНА СИСТЕМА НА ОСНОВІ ГЕКСАКОПТЕРА ДЛЯ ВЗЯТТЯ ПРОБ ВОДИ З АДАПТИВНИМ ПЛАНУВАННЯМ МАРШРУТУ ТА КООРДИНАЦІЄЮ ДЕКІЛЬКОХ ДРОНІВ

Андрій Писаренко

Національний технічний університет України
«Київський політехнічний інститут імені Ігоря Сікорського», Київ, Україна
<http://orcid.org/0000-0001-7947-218X>

Олександр Ролік

Національний технічний університет України
«Київський політехнічний інститут імені Ігоря Сікорського», Київ, Україна
<http://orcid.org/0000-0001-8829-4645>

Об'єктом цього дослідження є кіберфізична система на базі гексакоптера, призначена для автономного відбору проб води з метою моніторингу довкілля, що вирішує проблему ефективності керування в динамічних умовах. Предмет дослідження фокусується на інтеграції фізичного керування польотом та операцій з відбору проб води з плануванням місій на кіберрівні, включаючи навігацію по точках маршруту в режимі реального часу, планування завдань та координацію декількох дронів. Дослідження аналізує продуктивність системи за різних варіантів корисного навантаження та вітрових перешкод, забезпечуючи надійність та точність у несприятливих умовах. Метою дослідження є підвищення ефективності відбору проб води за допомогою кіберфізичної системи, досягнення підвищеної стійкості польоту та точності позиціонування за допомогою каскадної системи керування, оптимізація планування місій за допомогою адаптивних кіберстратегій та підвищення масштабованості за рахунок використання декількох дронів. Цей підхід спрямований на те, щоб перевершити традиційні системи БПЛА за допомогою фізично-кібернетичної інтеграції для точної, надійної та масштабованої оцінки якості води.

Методологія поєднує моделювання та аналітичні методи для створення та оцінки кіберфізичної системи на основі гексакоптера. У MATLAB/Simulink побудована математична модель із 6 ступенями свободи на основі рівнянь Ньютона-Ейлера для моделювання динаміки гексакоптера з урахуванням корисного навантаження та впливу вітру. Каскадна система керування розроблена з використанням MATLAB/Simulink, коефіцієнти якої налаштовані за допомогою методу Зіглера-Ніколса, після чого проведена ітеративна оптимізація для мінімізації перерегулювання та часу стабілізації в трьох сценаріях: 1 кг статичного корисного навантаження, 1,5 кг динамічного корисного навантаження та вітер 5 м/с. Кіберфізична компонента, реалізована в ROS 2, використовує алгоритми на основі графів (Дейкстра для навігації по точках маршруту, лістинг-планування для розподілу завдань) та протокол консенсусу для координації декількох дронів, випробуваний в середовищі розміром 500x500 м². Для оцінки ефективності системи проаналізовані такі показники продуктивності як середньоквадратична похибка положення (RMSE) та похибки орієнтації.

Результати демонструють підвищення можливостей відбору проб води. Каскадне керування дозволило зменшити середньоквадратичну похибку положення на 40–50% і утримувати похибки орієнтації в межах від $\pm 0.8^\circ$ до $\pm 1.2^\circ$ у всіх протестованих сценаріях, забезпечуючи точний і стабільний політ. Кіберфізична складова системи скоротила час виконання місії на 15% завдяки адаптивній оптимізації траєкторії, а координація декількох дронів збільшила зону відбору проб на 20%, підвищивши масштабованість. Ці результати відображають точність і надійність системи, що підкреслює нові стратегії керування та координації, які мають практичну цінність для моніторингу довкілля. Дослідження забезпечує основу для майбутніх екологічних застосувань.

Ключові слова: відбір проб води, кіберфізичні системи, моніторинг довкілля, координація кількох дронів, автономний безпілотний літальний апарат, планування місій.